

Phase transitions of the fast-ion conductor  $\text{K}_3\text{H}(\text{SeO}_4)_2$  studied by  $^1\text{H}$  and  $^{39}\text{K}$  NMR spectroscopy

This article has been downloaded from IOPscience. Please scroll down to see the full text article.

2006 J. Phys.: Condens. Matter 18 2173

(<http://iopscience.iop.org/0953-8984/18/7/006>)

View [the table of contents for this issue](#), or go to the [journal homepage](#) for more

Download details:

IP Address: 129.252.86.83

The article was downloaded on 28/05/2010 at 08:58

Please note that [terms and conditions apply](#).

# Phase transitions of the fast-ion conductor $\text{K}_3\text{H}(\text{SeO}_4)_2$ studied by $^1\text{H}$ and $^{39}\text{K}$ NMR spectroscopy

Ae Ran Lim<sup>1,3</sup> and M Ichikawa<sup>2,4</sup>

<sup>1</sup> Department of Science Education, Jeonju University, Jeonju 560-759, Korea

<sup>2</sup> Division of Physics, Graduate School of Science, Hokkaido University, Sapporo 060-0810, Japan

E-mail: [aeranlim@hanmail.net](mailto:aeranlim@hanmail.net) and [arlim@jj.ac.kr](mailto:arlim@jj.ac.kr)

Received 31 October 2005, in final form 8 January 2006

Published 2 February 2006

Online at [stacks.iop.org/JPhysCM/18/2173](http://stacks.iop.org/JPhysCM/18/2173)

## Abstract

The  $^1\text{H}$  and  $^{39}\text{K}$  spin–lattice relaxation,  $T_1$ , spin–spin relaxation time,  $T_2$  in the laboratory frame, and the spin–lattice relaxation time in the rotating frame  $T_{1\rho}$  in superionic  $\text{K}_3\text{H}(\text{SeO}_4)_2$  single crystals grown by the slow evaporation method were measured in the ferroelastic and paraelastic phases. The  $^1\text{H}$   $T_1$ ,  $T_{1\rho}$ , and  $T_2$  exhibited different trends with temperature in the ferroelastic phase, but were found to have very similar, liquid-like values in the paraelastic phase. In the paraelastic phase, the reorientational and translational motions are lost, and the proton motion can be characterized with a single correlation frequency,  $\omega_c$ . The observation that the variations of  $^1\text{H}$   $T_1$ ,  $T_{1\rho}$ , and  $T_2$  of  $\text{K}_3\text{H}(\text{SeO}_4)_2$  crystals with temperature are very similar in the paraelastic phase indicates that the destruction and reconstruction of hydrogen bonds does indeed occur at high temperatures. In addition, the  $^{39}\text{K}$   $T_1$  and  $T_2$  were found to be similar at high temperatures, as was also observed for the  $^1\text{H}$   $T_1$  and  $T_2$ . The crystal in the high-temperature phase is a fast ionic conductor. The motion giving rise to this liquid-like behaviour may be related to superionic motion.

## 1. Introduction

Hydrogen-bonded  $\text{M}_3\text{H}(\text{XO}_4)_2$  ( $\text{M} = \text{K}, \text{Rb}, \text{Cs}, \text{NH}_4$ ;  $\text{X} = \text{S}, \text{Se}$ ) crystals are well known for their high protonic conductivity, which increases significantly in the high-temperature superionic phases [1]. The conductivity of these crystals is associated with the dynamical disordering of the hydrogen-bond network, which results in an increase in the number of possible proton positions [2]. Proton conduction occurs in several types of materials, including many hydrogen-bonded systems [3–9]. Most crystals in the  $\text{M}_3\text{H}(\text{XO}_4)_2$  family undergo a superprotonic phase transition from a monoclinic room-temperature phase to a trigonal

<sup>3</sup> Author to whom any correspondence should be addressed.

<sup>4</sup> Present address: Kitanosawa 7-1-30, Minami-ku, Sapporo 005-0832, Japan.

high-temperature phase. In the vicinity of the phase transition temperature  $T_c$ , the electrical conductivity rapidly increases with temperature, and it is decreased by a power law for the temperature dependence. In the paraelastic phase above  $T_c$  the conductivity is exceedingly high, as high as that found in ionic conductors [10, 11]. At room temperature all the members of this family are ferroelastic and isomorphous with space group  $A2/a$ , except  $\text{Cs}_3\text{H}(\text{SeO}_4)_2$  with space group  $C2/m$  [12]. Above room temperature they undergo ferroelastic transitions in the range 339–456 K to trigonal ( $R3m$ ) paraelastic and superionic phases [13, 14].  $\text{K}_3\text{H}(\text{SeO}_4)_2$  belongs to a family of hydrogen-bonded crystals with the general formula  $\text{M}_3\text{H}(\text{XO}_4)_2$ .  $\text{K}_3\text{H}(\text{SeO}_4)_2$  undergoes two successive phase transitions at 20 and 390 K (the phases are denoted I, II, and III in descending order of temperature); it is antiferroelectric in phase III, ferroelastic in phase II, and exhibits high electrical conductivity in phase I [15]. The crystal structure of  $\text{K}_3\text{H}(\text{SeO}_4)_2$  at temperatures below 20 K has not yet been reported, and although its physical properties have been reported, other properties such as its nuclear magnetic resonance (NMR) have not yet been studied.

The spin–lattice relaxation time can be used as a measure of the dynamics of a crystal, such as the nucleus–phonon interaction, and indicates how readily the excited state energy of the nuclear system is transferred into the lattice. As protons are expected to play a dominant role in the physical properties and phase transition mechanisms of these hydrogen-bonded crystals, probing their proton motions with  $^1\text{H}$  NMR is expected to be a powerful means of studying their microscopic nature.  $\text{K}_3\text{H}(\text{SeO}_4)_2$  is important for studies of the correlation between transition temperatures and hydrogen bonding because of its low transition temperature. To obtain information about the structural phase transition and the relaxation processes that occur in  $\text{K}_3\text{H}(\text{SeO}_4)_2$  single crystals, it is useful to measure the spin–lattice relaxation time in the laboratory frame,  $T_1$ , the spin–lattice relaxation time in the rotating frame,  $T_{1\rho}$ , and the spin–spin relaxation time,  $T_2$ , for the  $^1\text{H}$  and  $^{39}\text{K}$  nuclei. The present study investigated the temperature dependences of  $T_1$ ,  $T_{1\rho}$ , and  $T_2$  for the  $^1\text{H}$  and  $^{39}\text{K}$  nuclei in  $\text{K}_3\text{H}(\text{SeO}_4)_2$  single crystals using a pulse NMR spectrometer. The motions of the  $^1\text{H}$  and  $^{39}\text{K}$  nuclei in the ferroelastic and paraelastic phases are discussed in the light of these results. The correlation between superionic motion and the relaxation times at high temperatures is discussed, for the first time.

## 2. Crystal structure

The monoclinic unit cell of the  $\text{K}_3\text{H}(\text{SeO}_4)_2$  crystal with space group  $A2/a$  at room temperature is characterized by lattice parameters  $a = 10.1291 \text{ \AA}$ ,  $b = 5.9038 \text{ \AA}$ ,  $c = 14.961 \text{ \AA}$ , and  $\beta = 103.64^\circ$  [16–18]. The crystal structure of the ferroelastic phase of  $\text{K}_3\text{H}(\text{SeO}_4)_2$  is shown in figure 1. The structure of  $\text{K}_3\text{H}(\text{SeO}_4)_2$  is built up of hydrogen-bonded  $\text{SeO}_4$  dimers and K cations. There are two kinds of K atom: K(1) occupies a special position on the twofold axis; K(2) is at a general position. Both types of K atom are surrounded by ten oxygen atoms. A given  $\text{SeO}_4\text{--H--SeO}_4$  dimer consists of two slightly deformed  $\text{SeO}_4$  tetrahedra. The two  $\text{SeO}_4$  tetrahedra are connected by a hydrogen bond. The crystal structure of the paraelastic phase belongs to the space group  $R3m$  with  $a = 6.118 \text{ \AA}$  and  $c = 22.629 \text{ \AA}$ . In this case, the crystal is characterized by rhombohedral symmetry with a unit cell in the hexagonal structure.

## 3. Experimental method

Single crystals of  $\text{K}_3\text{H}(\text{SeO}_4)_2$  were prepared by cooling from around 313 K a saturated aqueous solution containing excess selenic acid compared with its stoichiometric amount; the molar ratio of  $\text{K}_2\text{SeO}_4\text{:H}_2\text{SeO}_4$  was 3:1.54. The crystals obtained are hexagonal

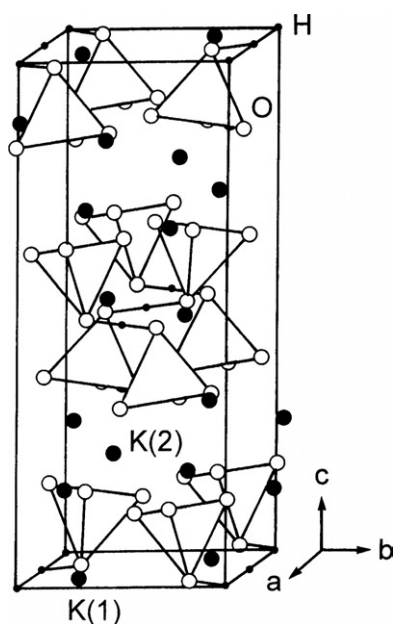


Figure 1. Projection of the  $K_3H(SeO_4)_2$  crystal at room temperature.

thin plates, similar to the pseudo-hexagonal  $c$ -plates of  $K_3H(SO_4)_2$ , but sometimes exhibit twinning [19, 20]. Transparent plates with dominant (001) faces were obtained.

The NMR signals of the  $^1H$  and  $^{39}K$  nuclei in the  $K_3H(SeO_4)_2$  single crystals were measured using Varian 200 FT NMR and Bruker DSX 400 FT NMR spectrometers, respectively, at the Korea Basic Science Institute. The static magnetic fields were 4.7 and 9.4 T respectively, and the central radio frequency was set at  $\omega_0/2\pi = 200$  MHz for the  $^1H$  nucleus and at  $\omega_0/2\pi = 18.67$  MHz for the  $^{39}K$  nucleus. The  $^1H$  and  $^{39}K$  experiments were performed using a  $\pi-t-\pi/2$  pulse sequence for the  $T_1$  measurements, a spin-locking sequence  $\pi-B_1(t)$  with  $B_1 = 5$  kHz for the  $T_{1\rho}$  measurements, and the  $T_2$  were measured using the solid echo method. The temperature-dependent NMR measurements were obtained over the temperature range 160–450 K. The samples were maintained at a constant temperature (accuracy,  $\pm 0.5$  K) by controlling the helium gas flow and the heater current.

## 4. Experimental results and discussion

### 4.1. $^1H$ NMR in $K_3H(SeO_4)_2$ crystals

The temperature dependences of  $T_1$ ,  $T_{1\rho}$ , and  $T_2$  for protons, when the static magnetic field is applied along the crystallographic  $c$ -axis, are shown in figure 2. The spin-lattice relaxation time in the laboratory frame,  $T_1$ , was measured using an inversion recovery sequence. The spin-spin relaxation time,  $T_2$ , was determined with the solid echo method, and exhibits a strong temperature dependence. In the ferroelastic phase,  $T_1$  differs from  $T_{1\rho}$ , which is in turn different from  $T_2$ , although they converge to similar values in the paraelastic phase. In the ferroelastic phase,  $T_1$  and  $T_{1\rho}$  are not governed by the same mechanism.  $T_1$  is determined by the relatively fast  $HSeO_4$  rotational reorientations, whereas  $T_{1\rho}$  is determined by proton translational motion, which is much slower. The slow translational jumps of protons result in

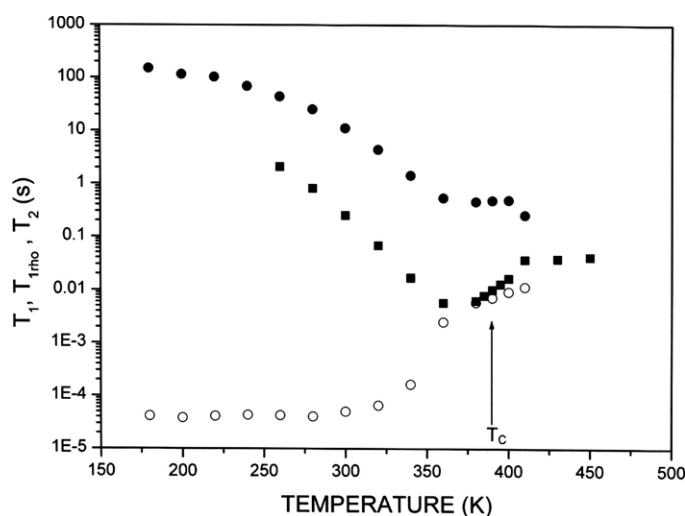


**Figure 2.** Temperature dependences of the spin–lattice relaxation time in the laboratory frame,  $T_1$ , spin–lattice relaxation time in the rotating frame,  $T_{1\rho}$ , and spin–spin relaxation time,  $T_2$ , for  $^1\text{H}$  in a  $\text{K}_3\text{H}(\text{SeO}_4)_2$  single crystal (●:  $T_1$ , ■:  $T_{1\rho}$ , and ○:  $T_2$ ).

a minimum in the variation of  $T_{1\rho}$  with temperature. The minimum in  $T_{1\rho}$  was found to occur at 360 K, for  $\omega_1\tau_c = 1$  at 5.7 ms. At low temperatures, the proton NMR free induction decay is short, indicative of a rigid lattice. As the temperature increases,  $\omega_c$  (reorientation) speeds up, resulting in a narrowing of the proton NMR line-width and, as a result,  $T_2$  increases. This increase in  $T_2$  is due to the rapid motion of the protons between the oxygens of each  $\text{SeO}_4$  group, giving rise to different, well-defined ‘orientations’ of the  $\text{H}(\text{SeO}_4)_2^{3-}$  ion. Above 390 K, the  $^1\text{H}$   $T_1$ ,  $T_{1\rho}$ , and  $T_2$  become liquid-like, indicating the presence of translational motion in addition to molecular ‘rotation’. The observation of liquid-like values of the proton  $T_1$ ,  $T_{1\rho}$ , and  $T_2$  is compatible with the suggestion that the phase above  $T_c$  is superionic. This is consistent with the appearance of a ‘liquid-like’ value of proton  $T_2$  in  $(\text{NH}_4)_4\text{LiH}_3(\text{SeO}_4)_4$  and  $(\text{NH}_4)_4\text{LiH}_3(\text{SO}_4)_4$  as discussed by Blinc *et al* [21]. The liquid-like  $T_2$  value indicates a drastic motional averaging of the proton dipole–dipole interactions due to translational motion, and is characteristic of a superionic state. At temperatures above the phase transition temperature, the crystal lattice changes significantly. This is demonstrated by the change in the proton  $T_1$  and  $T_2$ . The ferroelastic phase is characterized by a correlation time for reorientational motions that is shorter than the correlation time for translational motions. At high temperatures, the reorientational and translational motions are lost, and the proton motion can be characterized with a single correlation frequency  $\omega_c$ . From the temperature dependences of  $T_1$  and  $T_2$ , we conclude that, in the ferroelastic phase,  $\omega_{\text{dip}} \ll \omega_c$  (reorientation)  $< \omega_0$ . Here  $\omega_{\text{dip}}$  is the proton Larmor frequency in the local dipolar field (i.e., the dipolar width of the proton line expressed in frequency units),  $\omega_c$  (reorientation) is the frequency of the rotational motions of the  $\text{H}(\text{SeO}_4)_2$  group between different equilibrium orientations,  $\omega_c$  (translation) is the frequency of the motions of the protons between different sites due to translational motion, and  $\omega_0$  is the Larmor frequency in the external magnetic field.

#### 4.2. $^{39}\text{K}$ NMR in $\text{K}_3\text{H}(\text{SeO}_4)_2$ crystals

We now discuss the recovery laws for quadrupole relaxation for a nuclear spin system of  $^{39}\text{K}$  ( $I = 3/2$ ). The transition probabilities for  $\Delta m = \pm 1$  and  $\Delta m = \pm 2$  are  $W_1$  and  $W_2$ ,

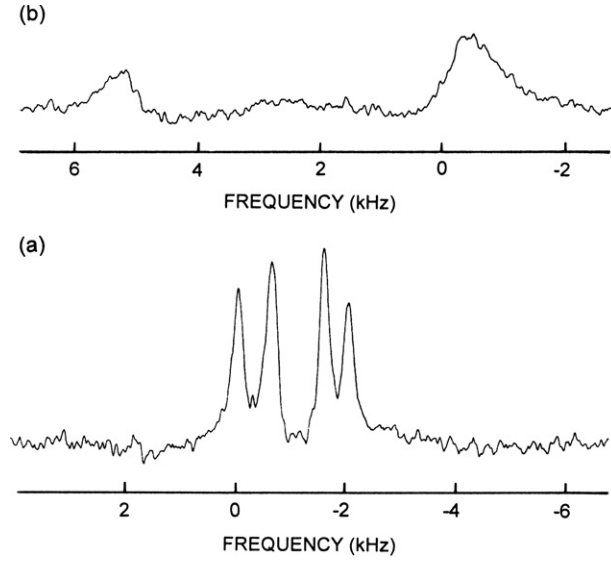


**Figure 3.**  $^{39}K$  NMR spectrum of a  $K_3H(SeO_4)_2$  single crystal (a) below  $T_c$  and (b) above  $T_c$ .

respectively. The rate equations are then as follows [22]:

$$\begin{aligned}
 dn_{-3/2}/dt &= -(W_1 + W_2)n_{-3/2} + W_1n_{-1/2} + W_2n_{1/2}, \\
 dn_{-1/2}/dt &= -W_1n_{-3/2} - (W_1 + W_2)Wn_{-1/2} + W_2n_{3/2}, \\
 dn_{1/2}/dt &= W_2n_{-3/2} - (W_1 + W_2)Wn_{1/2} + W_1n_{3/2}, \\
 dn_{3/2}/dt &= W_2n_{-1/2} + W_1n_{1/2} - (W_1 + W_2)n_{3/2}
 \end{aligned} \tag{1}$$

where  $n_{-3/2}$ ,  $n_{-1/2}$ ,  $n_{1/2}$ , and  $n_{3/2}$  are the differences in population between the equilibrium value and that at time  $t$  for each energy level. The eigenvalues of these equations are  $W_1$ ,  $W_2$ , and  $W_1 + W_2$ .

When the central line is at saturation, the recovery function for the central line is calculated to be [23, 24]

$$S(\infty) - S(t) = 2S(\infty)[0.5 \exp(-2W_1t) + 0.5 \exp(-2W_2t)] \tag{2}$$

where  $S(t)$  is the nuclear magnetization corresponding to the central transition at time  $t$  after saturation. The spin-lattice relaxation rate,  $1/T_1$ , is given by [25, 26]

$$1/T_1 = [2(W_1 + 4W_2)]/5 \tag{3}$$

The  $^{39}K$  NMR spectrum has three resonance lines as a result of the quadrupole interactions of the  $^{39}K$  ( $I = 3/2$ ) nucleus. When the crystal is rotated about the crystallographic axis, crystallographically equivalent nuclei give rise to three lines: one central line and two satellite lines. Instead of three resonance lines for the  $^{39}K$  nucleus in  $K_3H(SeO_4)_2$  crystals, four resonance lines are obtained in the temperature range 180–380 K, as shown in figure 3(a). The magnitudes of the quadrupole parameters of  $^{39}K$  nuclei are of the order of megahertz, so usually only central lines are obtained. The four resonance lines are obtained for the central transition ( $+1/2 \leftrightarrow -1/2$ ) of the  $^{39}K$  NMR spectrum. This result points to the presence of two types of crystallographically inequivalent  $^{39}K$  nuclei, K(1) and K(2). The four resonance lines are due to the existence of two kinds of ferroelastic domain. Above 390 K, two resonance lines corresponding to the crystallographically inequivalent K(1) and K(2) nuclei are obtained,

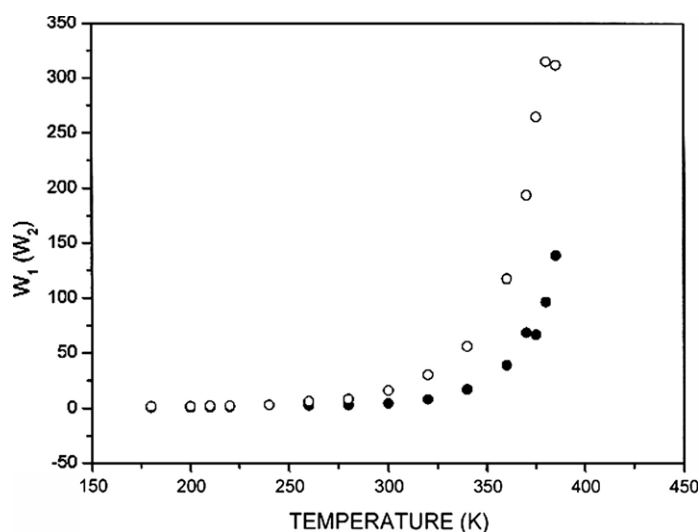


**Figure 4.** Temperature dependences of the  $^{39}\text{K}$  spin-lattice transition rates  $W_1$  and  $W_2$  of a  $\text{K}_3\text{H}(\text{SeO}_4)_2$  single crystal (●:  $W_1$  and ○:  $W_2$ ).

as shown in figure 3(b). The change to two resonance lines from four resonance lines is associated with the phase transition at 390 K, which indicates that the ferroelastic character has disappeared. The linewidth is broader above  $T_c$  than below  $T_c$ , and the broad linewidth at high temperatures is averaged out by motion in the high-temperature phase. Also, the splitting at high temperature is larger than at low temperature, i.e., 6 kHz instead of 2 kHz. The change of the splitting of the  $^{39}\text{K}$  resonance line in the phase transition temperature of 390 K means that the electric field gradient (EFG) at the  $^{39}\text{K}$  sites did change with temperature, which in turn means that the neighbouring atoms to the  $^{39}\text{K}$  did displace from their high-temperature positions.

The spin-lattice relaxation time,  $T_1$ , and the spin-spin relaxation time,  $T_2$ , for the four resonance lines of  $^{39}\text{K}$  in  $\text{K}_3\text{H}(\text{SeO}_4)_2$  were measured in the ferroelastic and paraelastic phases. The spin-lattice relaxation times were obtained with the inversion recovery method. The recovery traces for the four resonance lines of  $^{39}\text{K}$  with dominant quadrupole relaxation can be expressed as a linear combination of two exponential functions, as in equation (2). The  $^{39}\text{K}$  relaxation rates  $W_1$  and  $W_2$  of  $\text{K}_3\text{H}(\text{SeO}_4)_2$  in the ferroelastic phase are shown in figure 4, where  $W_1$  is smaller than  $W_2$ , and  $W_1$  and  $W_2$  exhibit similar temperature dependences. The  $^{39}\text{K}$   $W_1$  and  $W_2$  of  $\text{K}_3\text{H}(\text{SeO}_4)_2$  increase monotonically with temperature up to 350 K, and at high temperatures the relaxation rate increases rapidly with temperature. This trend is similar to that of  $^{39}\text{K}$  in the  $\text{KHSeO}_4$  crystal [27]. The nuclear spin-lattice relaxation time,  $T_1$ , for  $^{39}\text{K}$  was obtained using equation (3) in terms of  $W_1$  and  $W_2$ , and the results are shown in figure 5. The variations with temperature of  $T_1$  for the four resonance lines of K are very similar, and their values are the same within experimental error. Further, the spin-spin relaxation time,  $T_2$ , was determined for each line, and was found to depend on temperature.  $T_2$  increases with increasing temperature, and near 320 K starts to decrease with temperature, as shown in figure 5. Above 390 K, the spin-lattice relaxation time and the spin-spin relaxation time abruptly decrease, and converge to similar values. This is consistent with the trend of  $^{123}\text{Sb}$   $T_1$  and  $T_2$  in  $\text{K}_2\text{SbF}_5$  studied by Panich *et al* [28]. The relaxation times above  $T_c$  show values in the range expected for a fast-ion conductor with liquid-like particle motion. The spin-lattice relaxation time of  $^1\text{H}$

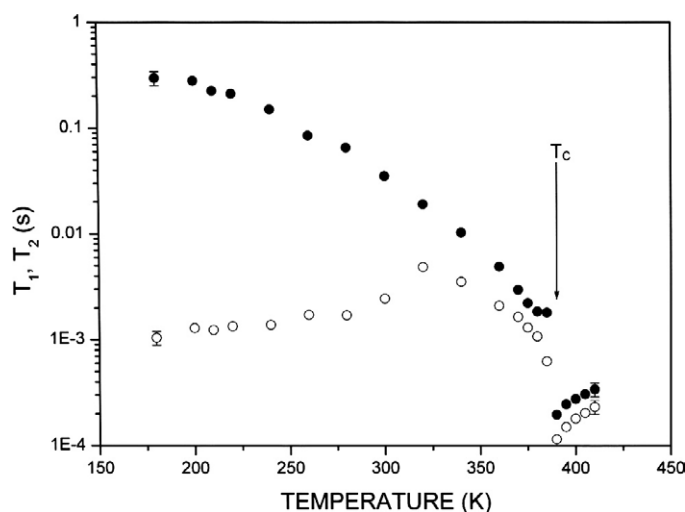


**Figure 5.** Temperature dependences of the spin–lattice relaxation time,  $T_1$ , and spin–spin relaxation time,  $T_2$ , of  $^{39}\text{K}$  in a  $\text{K}_3\text{H}(\text{SeO}_4)_2$  single crystal (●:  $T_1$  and ○:  $T_2$ ).

was found to be longer than that of  $^{39}\text{K}$ . It is expected that the potassium nuclei will relax more quickly than protons due to their quadrupolar moment.

## 5. Conclusion

The spin–lattice relaxation time,  $T_1$ , and the spin–spin relaxation time,  $T_2$ , in the laboratory frame, and the spin–lattice relaxation time in the rotating frame,  $T_{1\rho}$ , for the  $^1\text{H}$  and  $^{39}\text{K}$  nuclei in  $\text{K}_3\text{H}(\text{SeO}_4)_2$  single crystals were investigated with NMR spectrometer. These NMR observations provide a consistent description of the dynamics of the  $^1\text{H}$  and  $^{39}\text{K}$  nuclei in this material. Below  $T_c$ ,  $T_1$  differs from  $T_{1\rho}$ , which is in turn different from  $T_2$ , although they converge to similar values above  $T_c$ . Near 390 K,  $T_1$ ,  $T_{1\rho}$ , and  $T_2$  for  $^1\text{H}$  are similar, and are indicative of a liquid-like system, with both translational motion and molecular ‘rotation’ present. At high temperatures where the  $\text{HSeO}_4^-$  reorientations speed up and, because of translational motion, the structure becomes near isotropic, the width of the local polarization distribution and of the correlation time distribution diminish significantly, and the material becomes progressively more plastic. The liquid-like values of  $T_1$ ,  $T_{1\rho}$ , and  $T_2$  indicate that the phase above  $T_c$  ( $\approx 390$  K) is superionic. The structural phase transition at high temperatures may involve the breaking of hydrogen bonds between the nearest  $\text{SeO}_4$  and the forming of new weaker disordered hydrogen bonds between neighbouring  $\text{SeO}_4$  tetrahedra. This structural phase transition may involve significant reorientation of  $\text{SeO}_4$  tetrahedra and dynamical disorder of the hydrogen bonds between them. According to previous reports [29, 30], the high electrical conductivity of the superionic phase of  $\text{M}_3\text{H}(\text{XO}_4)_2$  ( $\text{M} = \text{K}, \text{Rb}, \text{Cs}, \text{and } \text{NH}_4$ ) crystals is due to the hopping of protons, which is accompanied by the destruction and reconstruction of hydrogen bonds. A short spin–lattice relaxation time at high temperatures is consistent with the destruction of hydrogen bonds. In the case of  $\text{K}_3\text{H}(\text{SeO}_4)_2$  crystals, the  $^1\text{H}$  spin–lattice relaxation time decreases with increasing temperature, indicating that the destruction and reconstruction of hydrogen bonds does occur at high temperatures. The variations of the  $^{39}\text{K}$   $T_1$  and  $T_2$  with temperature are similar to those observed for the  $^1\text{H}$   $T_1$ ,  $T_{1\rho}$ , and  $T_2$ . The crystal in the high-temperature phase is a fast ionic conductor. This behaviour



is expected for most hopping-type ionic conductors, and could be attributed to interactions between the mobile ions and the neighbouring group ions within the crystal. The potassium atoms are not involved in this type of dynamics. However, the spin interactions determining the relaxation times for both  $^1\text{H}$  and  $^{39}\text{K}$  nuclei are probably coupled, which means that the dynamics of the protons influence the dipolar and quadrupolar interactions controlling the relaxation time of the  $^{39}\text{K}$  nuclei. This explains the similar trend in the relaxation times determined from NMR data in the  $^1\text{H}$  and  $^{39}\text{K}$  NMR experiments.

## Acknowledgment

This work was supported by a Korea Research Foundation Grant (KRF-2004-015-C00148).

## References

- [1] Haile M, Boysen D A, Chisholm C R and Merle R B 2001 *Nature* **410** 910
- [2] Pavlenko N I 1999 *J. Phys.: Condens. Matter* **11** 5099
- [3] Kawada A, McGhie A R and Labes M M 1970 *J. Chem. Phys.* **52** 3121
- [4] Schmidt V H, Drumheller J E and Howell F L 1971 *Phys. Rev. B* **4** 4582
- [5] Baranov A I, Shuvalov L A and Schagina N M 1982 *JEPT Lett.* **36** 459
- [6] Baranov A I, Fedosyuk R M, Schagina N M and Shuvalov L A 1984 *Ferroelectr. Lett.* **2** 25
- [7] Blinc R, Dolinsek J, Lahajnar G, Zupancic I, Shuvalov L A and Baranov I A 1984 *Phys. Status Solidi b* **123** k83
- [8] Friesel M, Baranowski B and Lunden A 1989 *Solid State Ion.* **35** 85
- [9] Baranov A I, Merinov B V, Tregubchenko A V, Khiznichenko V P, Shuvalov L A and Schagina N M 1989 *Solid State Ion.* **36** 279
- [10] Matsumoto Y 2001 *J. Phys. Soc. Japan* **70** 1437
- [11] Baranov A I, Tregubchenko A V, Shuvalov L A and Schagina N M 1987 *Fiz. Tverd. Tela* **29** 2513
- [12] Ichikawa M, Gustafsson T and Olovsson I 1991 *Solid State Commun.* **78** 547
- [13] Baranov A I, Tregubchenko A V, Shuvalov L A and Schagina N M 1987 *Sov. Phys.—Solid State* **29** 1448
- [14] Merinov B V, Baranov A I and Shuvalov L A 1990 *Sov. Phys.—Crystallogr.* **35** 200
- [15] Endo M, Kaneko T, Osaka T and Makita Y 1983 *J. Phys. Soc. Japan* **52** 3829
- [16] Ichikawa M, Sata S, Komukae M and Osaka T 1992 *Acta Crystallogr. C* **48** 1569
- [17] Ichikawa M, Gustafsson T and Olovsson I 1994 *Acta Crystallogr. C* **50** 330
- [18] Yamamura N O, Yamamura O, Matsuo T, Ichikawa M, Ibberson R M and David W I F 2000 *J. Phys.: Condens. Matter* **12** 8559
- [19] Yokota S, Makita Y and Takagi Y 1982 *J. Phys. Soc. Japan* **51** 1461
- [20] Chen R H, Chang R Y and Shern S C 2002 *J. Phys. Chem. Solids* **63** 2069
- [21] Blinc R, Lahajnar G, Seliger J, Zupancic I, Zimmermann M, Fuih A, Schranz W and Warhanek H 1994 *Solid State Commun.* **92** 765
- [22] Igarashi M, Kitagawa H, Takahashi S, Yoshizak R and Abe Y 1992 *Z. Naturf. a* **47** 313
- [23] Bonera G, Borsa F and Rigamonti A 1970 *Phys. Rev. B* **21** 2784
- [24] Towta S and Hughes D G 1990 *J. Phys.: Condens. Matter* **2** 2021
- [25] van der Klink J J, Rytz D, Borsa F and Hochli U T 1983 *Phys. Rev. B* **27** 89
- [26] Kim K H, Torgeson D R, Borsa F and Martin S W 1996 *Solid State Ion.* **90** 29
- [27] Lim A R, Yun I H and Yoon C S 2005 *Solid State Commun.* **134** 183
- [28] Panich A M, Zemnukhova L A and Davidovich R L 2001 *J. Phys.: Condens. Matter* **13** 1609
- [29] Matsumoto Y 1998 *J. Phys. Soc. Japan* **67** 2215
- [30] Matsuo Y, Hatori J, Nakashima Y and Ikehata S 2004 *Solid State Commun.* **130** 269